

Giant magnetoresistance in Cu-Mn-Al

L. Yiping, A. Murthy, and G. C. Hadjipanayis

Department of Physics and Astronomy, University of Delaware, Newark, Delaware 19716

H. Wan

Center for Magnetic Recording Research, University of California—San Diego, La Jolla, California 92093-0401

(Received 3 January 1996)

Giant negative magnetoresistance (GMR) has been observed in melt-spun $\text{Cu}_x\text{Mn}_y\text{Al}_z$ ribbons ($x=50-65$, $y=5-25$, and $z=25-30$), with values up to 15% at 30 K. GMR was observed in all samples with off-stoichiometric composition which had a tweed structure consisting of a mixture of Mn-rich and Mn-poor Cu_2MnAl -type (2:1:1) regions and/or of a fine mixture of magnetic 2:1:1 and nonmagnetic Cu_9Al_4 (9:4) phases. The highest value was obtained in samples with the 2:1:1 phase as a majority phase. The observed GMR is attributed to interfacial scattering at these fine structural mixtures. [S0163-1829(96)02930-X]

Recently, great attention has been focused on the giant negative magnetoresistance behavior of multilayered thin films,¹⁻³ granular systems,^{4,5} and melt-spun ribbons consisting of (Fe, Co, Ni)/(Ag, Au, Cu). Modeling of the giant magnetoresistance (GMR) has emphasized spin-dependent scattering at the interfacial regions between the ferromagnetic and nonmagnetic minority regions.^{6,7} In granular systems with GMR, the volume fraction of magnetic particles is below the percolation threshold, leading to isolated granules

in a nonmagnetic matrix with the granular size being comparable to, or smaller than, the electron mean free path. Above the percolation threshold, the size of the magnetic particles is increased above the mean free path, leading to a decreased surface/volume ratio with a subsequent reduction in the interfacial scattering and GMR.

We have recently observed a different GMR behavior in a melt-spun Cu-Mn-Al system where the magnetic phase is the majority phase, Cu-Mn-Al Heusler alloys have been extensively studied in the past because of their magnetic hardening behavior.^{8,9} High coercivities have been observed in some as-cast Cu-Mn-Al alloys with composition in the range between the Heusler phase, Cu_2MnAl (2:1:1) and the κ phase.⁸ Magnetic hardening has been attributed to domain wall pinning by nonmagnetic precipitates in a ferromagnetic matrix,¹⁰ and more recently¹¹ to a single-domain particle behavior, where noninteracting Cu_2MnAl particles are embedded in the nonmagnetic Cu_9Al_4 (9:4) matrix phase.

Our studies on Cu-Mn-Al showed GMR in a wide range of compositions. Values greater than 10% have been obtained in samples having a nearly single ferromagnetic 2:1:1

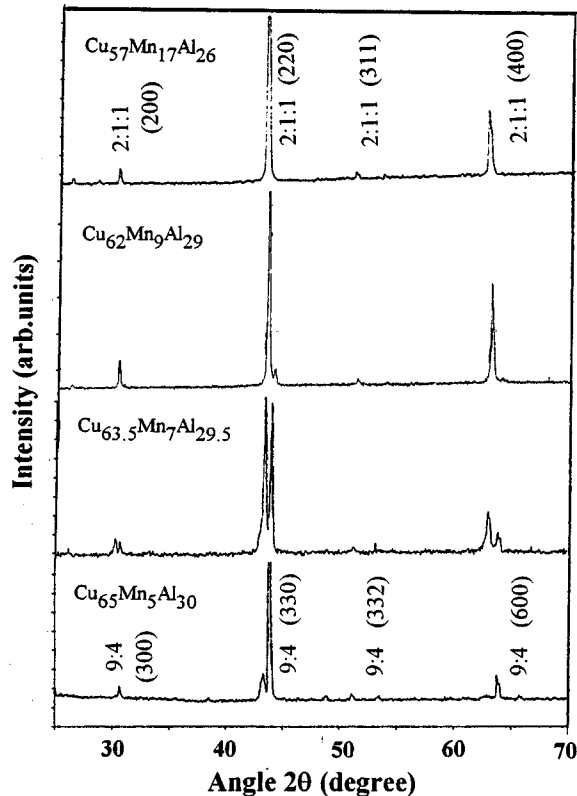


FIG. 1. X-ray diffraction patterns of Cu-Mn-Al ribbons with different compositions.

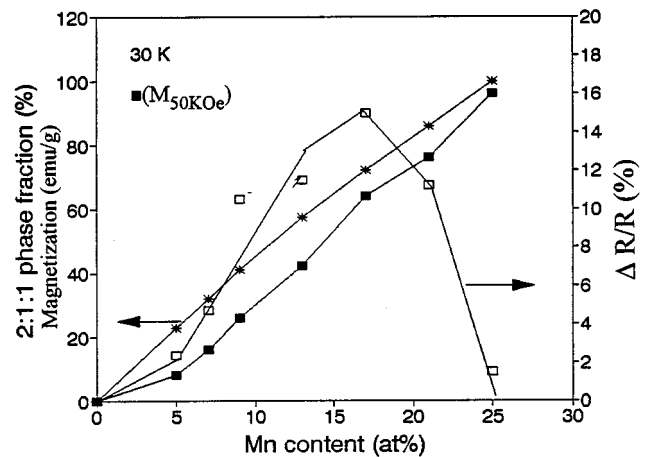


FIG. 2. Estimated 2:1:1 volume fraction, magnetization, and GMR as a function of Mn content.

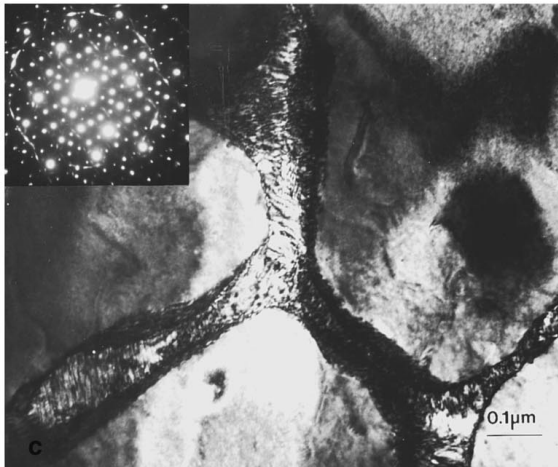
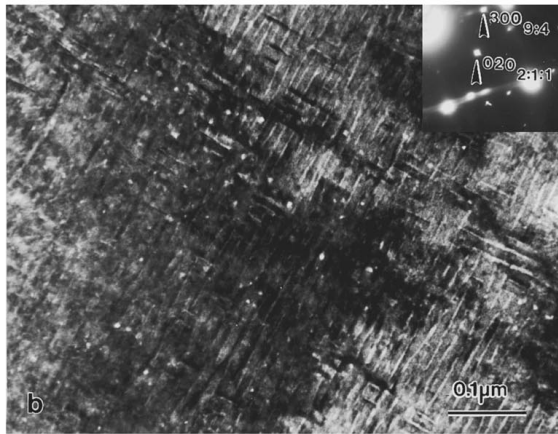
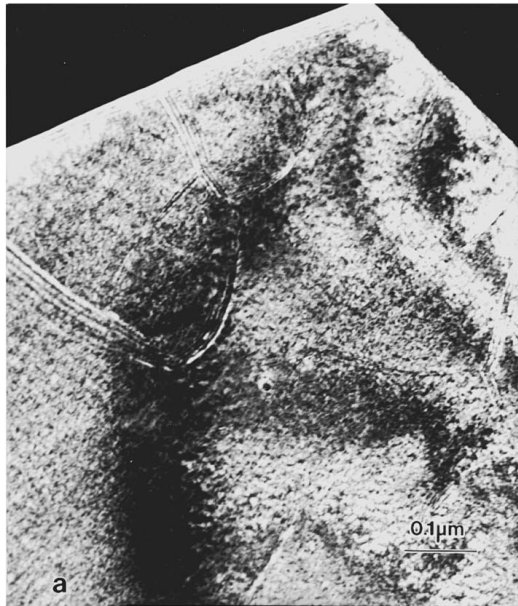


FIG. 3. GMR of Cu-Mn-Al ribbons as a function of (a) $\text{Cu}_{53}\text{Mn}_{21}\text{Al}_{26}$, (b) $\text{Cu}_{57}\text{Mn}_{17}\text{Al}_{26}$, and (c) $\text{Cu}_{65}\text{Mn}_5\text{Al}_{30}$.

phase and in samples with mixed 2:1:1 and 9:4 phases. An attempt was made to understand the origin of GMR by correlating the magnetic properties with the sample composition and microstructure.

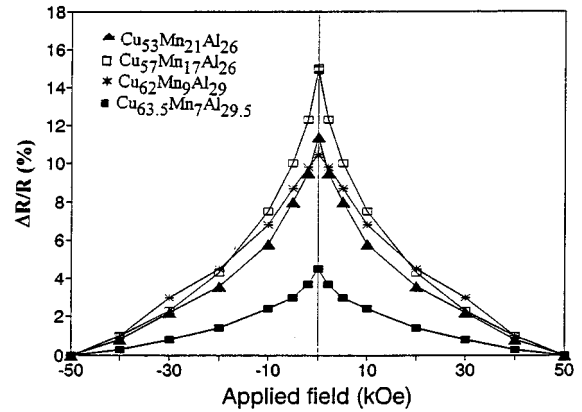


FIG. 4. GMR of Cu-Mn-Al ribbons as a function of applied field.

Cu-Mn-Al alloys were made by arc-melting the pure elements under an argon atmosphere. The Cu-Mn-Al ribbons were prepared by melt-spinning, using different quenching rates by varying the wheel speed. The samples were carefully prepared to ensure compositions closed to the nominal composition. The thickness of the ribbons was found to be in the range between 8 and 50 μm . The structure of all the samples was characterized by x-ray diffraction (XRD). The magnetic properties were measured by both a vibrating sample magnetometer (VSM) and a superconducting quantum interference device (SQUID) magnetometer in fields up to 50 kOe and in the temperature range of 10–700 K. The electrical resistivity $\rho(H, T)$ measurements were carried out using a dc four-point probe, where the fields were applied along the ribbon length and parallel to the current. Transmission electron microscopy (TEM) and energy dispersive x-ray analysis were used to study the microstructure and chemical composition of the samples, respectively.

Only a small magnetoresistance (about 1.5%) was observed in samples with the stoichiometric composition $\text{Cu}_{50}\text{Mn}_{25}\text{Al}_{25}$ which had a single Cu_2MnAl phase.

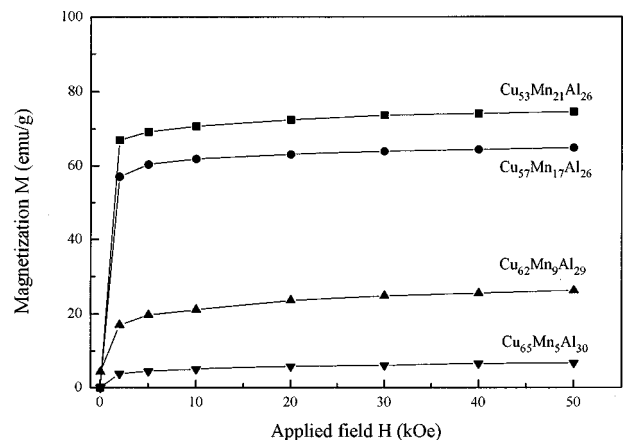


FIG. 5. Magnetization curves of Cu-Mn-Al ribbons with different compositions.

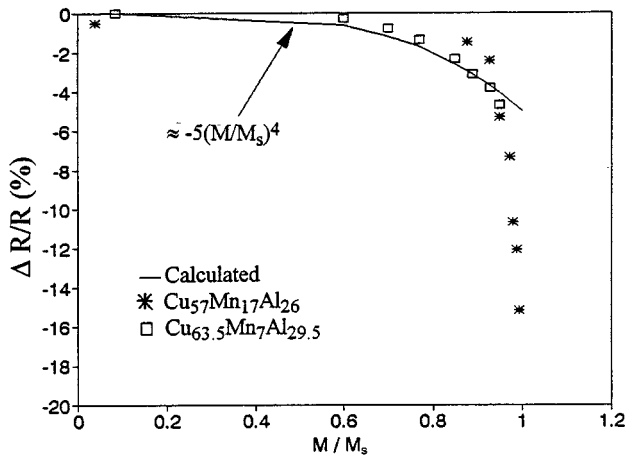


FIG. 6. Magnetoresistance $\Delta R/R(0)$ vs magnetization at 30 K.

$\text{Cu}_x\text{Mn}_y\text{Al}_z$ compositions were chosen so that their microstructure consisted of a mixture of ferromagnetic 2:1:1 and nonmagnetic Cu_9Al_4 phases that can lead to interfacial scattering, similar to that in other systems.^{12,13} By gradually decreasing the Mn content, the ratio of the 2:1:1 and 9:4 phases could be adjusted. This was achieved by varying the composition of $\text{Cu}_x\text{Mn}_y\text{Al}_z$ and keeping a constant ratio of $(x-27)/(z-y) \approx 2.2-2.5$ close to the Cu_9Al_4 composition ($\text{Cu}/\text{Al} \approx 2.2-2.5$).

Figure 1 shows the x-ray diffraction patterns of samples with a different ratio of the two phases: With decreasing Mn content the 9:4 phase gradually becomes a majority phase at the expense of the 2:1:1 phase. When the volume fraction of the 2:1:1 phase is greater than 60%, only a single 2:1:1 phase is observed in the x-ray diffraction patterns. This may imply that the size of 9:4 is too small and that they are randomly oriented. Also there was no shift in the XRD peaks, implying that the lattice parameters and hence the unit cell of the Cu_2MnAl phase remained the same in samples with different compositions. Figure 2 shows the estimated 2:1:1 volume fraction and $\Delta R/R(0)$ as a function of Mn content. GMR was readily observed in samples with off-stoichiometric composition. Values of $\Delta R/R(0)$ above 10% were easily obtained in samples with a structure consisting of a mixture of 9:4 and 2:1:1 phases, but with the latter as the majority phase. GMR reached a maximum value of 15% in a sample with 70% 2:1:1 phase and then gradually decreased in samples with the 9:4 phase as the majority phase. This behavior is different than that of other granular systems where the magnetic phase is the minority phase.

TEM studies on the samples with GMR showed three types of microstructure: (i) a tweed structure in samples with a majority 2:1:1 phase and 10% GMR [Fig. 3(a)], (ii) a fine mixture of 2:1:1 and 9:4 phases with the minority 9:4 phase sandwiched between the 2:1:1 phase plates with the highest GMR [Fig. 3(b)], and (iii) a mosaic structure consisting of

larger 9:4 grains surrounded by 2:1:1 clusters in samples with the 9:4 phase as the majority phase with 2.5% GMR [Fig. 3(c)].

The magnitude of GMR as a function of applied field is shown in Fig. 4. It may be noticed that GMR is strongly dependent on the sample's chemical composition and is not saturated even in a 50-kOe field. The corresponding magnetization curves of these samples are shown in Fig. 5. The magnetization of all the samples is close to saturation in contrast to the GMR. The magnetization is found to depend on the amount of Mn and therefore on the percentage of the ferromagnetic phase, decreasing almost linearly with the 2:1:1 phase. According to the two-current model,¹⁴ GMR can be expressed as $\rho(H) - \rho(0)/\rho(0) = -A(M/M_s)^2$, where the coefficient A is related to the magnitude of GMR. $\Delta R/R$ of the samples consisting of a fine mixture of 2:1:1 and 9:4 phases does not follow the $(M/M_s)^2$ relation (Fig. 6). This behavior is probably due to the fine nanocomposite structure of the samples which leads to large areas of randomly oriented surface spins that are pinned and therefore require high field to be saturated. Electrons are scattered primarily by these surface spins, and this leads to the nonsaturated GMR. The surface spins, however, constitute a small fraction of the total spins in the Cu_2MnAl phase, and this explains the close-to-saturation magnetization with a small high-field susceptibility as shown in Fig. 5. In samples with a slightly off-stoichiometric composition which show only a single 2:1:1 phase, the GMR observed is related to the tweed structure which develops prior to the precipitation of the 9:4 phase. In these samples, the off-stoichiometric composition leads to separation into Mn-rich and Mn-poor regions, all with the 2:1:1 structure. The Mn-poor regions can be assumed to be nonmagnetic, and hence this microstructure also leads to interfacial scattering. The tweed contrast observed in TEM [Fig. 3(a)] is due to the large strain induced in the lattice because of this composition separation.

In samples with the 9:4 phase as the majority matrix phase, a fine mixture of 2:1:1 and 9:4 phases occurs around the 9:4 large grains and this reduces the effective interfacial scattering and therefore the GMR. In these samples the magnetic entities are far apart, and this reduces the surface area and the surface anisotropy, leading to lower saturating fields of GMR.

In summary, giant negative magnetoresistance as high as 15% has been observed in Cu-Mn-Al ribbons. The highest GMR was observed in samples with a fine mixture of magnetic 2:1:1 and nonmagnetic 9:4 phases, but with the magnetic phase as the majority phase. However, high GMR was also obtained in a nearly single phase sample with a tweed microstructure consisting of Mn-rich and Mn-poor regions and in samples with the 9:4 as the majority phase, but with the magnetic clusters localized around large 9:4 grains. The observed GMR is far from saturation in contrast to the magnetization curves and is believed to be the result of interfacial scattering.

This work was supported by NSF Grant No. DMR 9307676.

- ¹M. N. Baibich, J. M. Broto, A. Fert, F. Nguyen Van Dan, F. Petroff, P. Elienne, B. Gruezer, A. Friederich, and J. Chazelas, *Phys. Rev. Lett.* **61**, 2472 (1988).
- ²J. J. Krebs, P. Lubitz, A. Chaiken, and G. A. Prinz, *Phys. Rev. Lett.* **63**, 1645 (1989).
- ³S. S. Parkin, N. More, and K. P. Roche, *Phys. Rev. Lett.* **64**, 2304 (1990).
- ⁴A. Berkowitz, A. P. Young, J. R. Mitchell, S. Zhang, M. J. Carey, F. E. Spada, F. T. Parker, A. Hütten, and G. Thomas, *Phys. Rev. Lett.* **68**, 3745 (1992).
- ⁵J. Q. Xiao, J. S. Jiang, and C. L. Chien, *Phys. Rev. Lett.* **68**, 3740 (1992).
- ⁶P. M. Levy and S. Zhang, *Phys. Rev. Lett.* **65**, 1643 (1990).
- ⁷R. E. Cawley and J. Barnas, *Phys. Rev. Lett.* **63**, 664 (1989).
- ⁸N. Karita and Y. Seloguchi, *Jpn. J. Appl. Phys.* **12**, 934 (1973).
- ⁹K. Narita and S. Koga, *Appl. Phys. Lett.* **41**, 712 (1977).
- ¹⁰S. Koga and K. Narita, *J. Appl. Phys.* **53**, 1655 (1982).
- ¹¹S. H. Aly, Y. J. Zhang, H. Wan, and G. C. Hadjipanayis, *J. Magn. Magn. Mater.* **130**, 297 (1994).
- ¹²C. L. Chien, J. Q. Xiao, and J. S. Jiang, *J. Appl. Phys.* **73**, 5309 (1993).
- ¹³A. E. Berkowitz, J. R. Mitchell, M. J. Carey, A. P. Young, D. Rao, A. Starr, S. Zhang, F. E. Spada, F. T. Parker, A. Hütten, and G. Thomas, *J. Appl. Phys.* **73**, 5320 (1993).
- ¹⁴S. Zhang, *Appl. Phys. Lett.* **61**, 1855 (1992).